

## Dynamic light scattering observation of droplet aggregation in a Winsor type W/O microemulsion system

Dag Waaler, Knut Arne Strand, Gunvald Stro/mme, and Torbjørn Sikkeland

Citation: *The Journal of Chemical Physics* **91**, 3360 (1989); doi: 10.1063/1.456910

View online: <http://dx.doi.org/10.1063/1.456910>

View Table of Contents: <http://scitation.aip.org/content/aip/journal/jcp/91/6?ver=pdfcov>

Published by the AIP Publishing

---

### Articles you may be interested in

[Synthesis and Characterization of Cholesterol Nano Particles by Using w/o Microemulsion Technique](#)  
AIP Conf. Proc. **1276**, 198 (2010); 10.1063/1.3504297

[Small-angle neutron scattering from giant water-in-oil microemulsion droplets. I. Ternary system](#)  
J. Chem. Phys. **128**, 054502 (2008); 10.1063/1.2779322

[Droplet density dependences of the static and dynamic structures in a ternary microemulsion system](#)  
AIP Conf. Proc. **708**, 92 (2004); 10.1063/1.1764069

[Dynamic universality in microemulsion system](#)  
AIP Conf. Proc. **256**, 320 (1992); 10.1063/1.42376

[Light scattering measurements in a dilute microemulsion](#)  
J. Chem. Phys. **84**, 5919 (1986); 10.1063/1.449904

---



**NEW Special Topic Sections**

**NOW ONLINE**  
Lithium Niobate Properties and Applications:  
Reviews of Emerging Trends

**AIP** | Applied Physics  
Reviews

# Dynamic light scattering observation of droplet aggregation in a Winsor type W/O microemulsion system

Dag Waaler<sup>a)</sup> Knut Arne Strand, Gunvald Strømme, and Torbjørn Sikkeland  
Physics Department, Norwegian Institute of Technology, 7034-Trondheim-NTH, Norway

(Received 24 March 1989; accepted 18 May 1989)

We have performed scattered light intensity autocorrelation measurements on a Winsor type microemulsion system composed of brine, cyclohexane, SDS and a mixture of 1-butanol and 1-pentanol. At high cosurfactant concentration, where the microemulsion phase was considered to consist of individual, spherical water-in-oil droplets of relatively low droplet volume fraction, the autocorrelation functions were observed to be essentially single exponential, as expected. Above a certain droplet volume fraction, however, *additional* decay modes were observed to enter the correlation data. These modes were interpreted to be due to rotation and/or internal motion of droplet aggregates.

## I. INTRODUCTION

Microemulsions are thermodynamically stable dispersions of oil and water,<sup>1</sup> with length scales of the surfactant stabilized internal oil and water microstructures typically of the order of 10 nm. Usually, the formation of proper microemulsions also requires addition of a second surfactant, termed cosurfactant,<sup>1</sup> and often salt as well.

The present work addresses the so-called Winsor microemulsion systems,<sup>2</sup> in which an oil-in-water (O/W) microemulsion coexisting with an excess oil-rich phase (Winsor I) can be continuously transformed into a water-in-oil (W/O) microemulsion in coexistence with an excess water-rich phase (Winsor II). This transformation can be driven by suitably changing a thermodynamic field of the system, e.g., salinity, temperature, pressure or chemical potential of the surfactants.<sup>1</sup> In the intermediate region, where the microemulsion consists of approximately equal water and oil volumes, the microemulsion coexists with both a water-rich and an oil-rich phase (Winsor III). Except in this middle region, where the internal microstructure is in some kind of bicontinuous state,<sup>3</sup> the microemulsions may be regarded as consisting of individual spherical droplets of brine (oil), coated with surfactant molecules, and suspended in a continuous phase of oil (brine).<sup>4</sup> Partially because of their potential use in enhanced oil recovery,<sup>5</sup> such Winsor systems have been extensively studied during the last decade.<sup>4</sup>

Dynamic light scattering (DLS) has been shown to be a very powerful tool for studying microemulsion systems.<sup>6</sup> Outside the bicontinuous domain the DLS data may be interpreted in terms of classical diffusion of the microemulsion droplets, and may thus provide information on droplet sizes and interactions. Furthermore, the DLS data may contain information pertaining to rotation and/or flexing motion of the scatterers<sup>7</sup> (i.e., microemulsion droplets or clusters of droplets).

Our work was motivated by the pioneering light scattering studies by Cazabat and Langevin,<sup>8</sup> in which they exam-

ined several dilute W/O microemulsions composed of brine, cyclohexane or toluene, sodium dodecyl sulfate (SDS), and either 1-butanol, 1-pentanol or 1-hexanol as cosurfactant. They found the droplet interactions to be strongly attractive in the microemulsions containing butanol, and much less attractive or even repulsive (in addition to excluded volume effects) in those containing pentanol or hexanol. To investigate the effect of particle interactions on the Winsor transition, we set out to study microemulsions with mixtures of 1-butanol and 1-pentanol as cosurfactant. The underlying idea was that this could allow us to tune the effective droplet interaction potential.

The present paper addresses the DLS results for a microemulsion with a 45% (mass) butanol/55% pentanol cosurfactant. In order to keep the salt concentration constant, we found it convenient to drive the transition by varying the total cosurfactant concentration of the system. In the following we shall first give a short account of the DLS theory relevant to the present work, then describe sample preparation and experimental procedures, and finally present and discuss the results.

## II. THEORETICAL BACKGROUND

The normalized field autocorrelation function of light scattered from  $N$  scatterers may be written<sup>7</sup>

$$g^{(1)}(q, t) = F(q, t)/S(q). \quad (1)$$

Here  $F(q, t)$  is the coherent intermediate scattering function,  $S(q) = F(q, 0)$  is the static structure factor and  $q$  is the scattering (or transfer) vector, defined as

$$q = \frac{4\pi n}{\lambda_0} \sin \theta / 2, \quad (2)$$

where  $n$  is the macroscopic refractive index of the sample,  $\lambda_0$  is the wavelength of light in vacuum, and  $\theta$  the scattering angle.

For noninteracting scatterers (particles, droplets) one has  $S(q) = 1$ , and  $F(q, t)$  is reduced to its self part  $F_s(q, t)$ , which for freely diffusing Brownian particles yields<sup>7</sup>

$$F_s(q, t) = e^{-D_0 q^2 t}. \quad (3)$$

<sup>a)</sup> Present address: Østlandsforskning, P. O. Box 430, N-2801 Gjøvik, Norway.

Here  $D_0$  is the free translational diffusion coefficient which for spherical particles may be related to a hydrodynamic radius  $R_H$  of the particle:

$$D_0 = \frac{kT}{6\pi\eta R_H}, \quad (4)$$

where  $\eta$  is the solvent bulk viscosity,  $k$  the Boltzmann constant, and  $T$  the absolute temperature of the system.

However, in the general case the scattered light also contains contributions due to particle anisotropy, polydispersity and interactions. The effect of these factors on  $F(q,t)$  are usually *separately* taken into account as follows:

For *nonspherical* (and/or optically anisotropic) scatterers with at least one dimension  $L > 3q^{-1}$ , the scattered spectrum may contain modes due to Brownian rotation/flexing motion of the scatterers.<sup>7</sup> In this case the self part of  $F(q,t)$  may be written as

$$F_s(q,t) = \sum_i S_i(qL) e^{-\Gamma_i t}, \quad (5)$$

where  $S_i(qL)$  is the dynamic form factor and  $\Gamma_i$  the decay constant on the  $i$ th mode.

Possible droplet size *polydispersity* may be taken into account by the standard method of cumulants,<sup>7</sup> where  $F_s(q,t)$  is expanded about the  $z$ -averaged diffusion coefficient  $\langle D_0 \rangle_z$ :

$$F_s(q,t) = e^{-\langle D_0 \rangle_z q^2 t} (1 + \frac{1}{2} \sigma^2 t^2 + \dots), \quad (6)$$

where  $\sigma^2$  is the variance in the diffusion coefficient distribution and thus is a measure of the degree of polydispersity.

And finally, considering *interactions* of the individual scatterers  $F(q,t)$  also will contain a coherent part  $F_c(q,t)$  due to correlations of the particle positions. For times  $t_b \ll t \ll t_i$ , where  $t_b$  is the time constant of the solvent molecular Brownian motions and  $t_i$  that of the interactions of the scatterers, one may formally replace  $D_0$  by an *effective* diffusion coefficient,  $D^{\text{eff}}$ :<sup>9</sup>

$$F(q,t) = F_s(q,t) + F_c(q,t) = e^{-D^{\text{eff}} q^2 t}. \quad (7)$$

### III. EXPERIMENTAL

The compositions of the examined microemulsions were as follows:

surfactant:	2% (weight of total) SDS (sodium dodecyl sulfate, p.A. > 99%, by Fluka AG)
cosurfactant:	varying concentration of a 45/55 weight mixture of 1-butanol and 1-pentanol (both p.A., Merck products)
oil:	cyclohexane (p.A. > 99.5% by Merck)
brine:	bidistilled water with 6 g/l NaCl (p.A. by Merck) (equal brine and oil volumes)

The cosurfactant concentrations were chosen to yield 12 different samples ranging from inside the Winsor III (three coexisting phases) into the Winsor II domain (W/O micro-

emulsion coexisting with a water-rich phase). The temperature was kept constant at  $(23.0 \pm 0.2)^\circ\text{C}$ , and the samples were repeatedly shaken until complete dissolution of the components were observed. Following equilibrium the relative phase volumes of the microemulsion and the excess phases were recorded. Extracts of the samples were transferred to the scattering cells keeping the original relative phase volumes approximately unchanged. As some of the samples were slightly turbid we used "time-glass" shaped scattering cells, with the scattering volume confined to the contracted part of the cell (diameter 1–2 mm).

In most of the experiments we used a low-noise 0.8 mW He-Ne laser (Spectra Physics 086-2,  $\lambda_0 = 632.8$  nm). For some of the less turbid samples the results were also checked using a Ar<sup>+</sup> laser (Spectra Physics 2020-5, max 3 W at  $\lambda_0 = 514.5$  nm). For each sample, the scattered intensity correlation function  $g^{(2)}(q,t)$  was recorded for 6–10 scattering angles in the range  $30^\circ$ – $150^\circ$ . The signal recordings and the data processings were performed using a photomultiplier (Malvern RF 320) and a 128 channel, 8 bits correlator (Malvern K 7032) connected to an Olivetti M24 Personal Computer.

The volume fraction  $\varphi$  of the water-rich droplets relative to the total microemulsion volume was taken to be

$$\varphi = \frac{V_w + V_s + V_c}{V_m}, \quad (8)$$

where  $V_w$ ,  $V_s$  and  $V_c$  are the brine, surfactant and cosurfactant volumes of the microemulsion droplets, respectively, and  $V_m$  the total volume of the microemulsion phase. In determining  $\varphi$  this way we have made the following assumptions:

- the SDS molecules are fully confined to the water–oil interphases, and thus  $V_s$  is equal to the total SDS volume.
- the aqueous content of the oil phase is negligible. (The aqueous concentration of the continuous (organic) phase in similar solutions has been determined to be 0.2%–0.4%,<sup>8</sup> and thus for  $\varphi > 10\%$ , as in the present case, this assumption is quite reasonable), and
- the cosurfactant concentration in the droplet cores equals that of the excess water-rich phase. This is called the pseudo-phase approximation, and is found to be reasonably well obeyed in microemulsions.<sup>8</sup>

Cosurfactant partitioning was obtained by combining the measured cosurfactant concentrations of the excess phase(s) using gas chromatography, and the knowledge of the total amount of cosurfactant added.

The gas chromatography equipment used consisted of a Shimadzu GC-MINI 3 with a Supelcowax 10 fused silica capillary column, and a Chromatopac C-R3A integrator, injector and (ionization) detector temperatures were kept constant at  $220^\circ\text{C}$ . The column temperature was set to  $60^\circ\text{C}$  at the time of the injection, and then programmed to raise  $10^\circ\text{C}/\text{min}$  during the measurement, a procedure which showed to yield distinct peak separations. Between each measurement the column was kept 2 min at  $140^\circ\text{C}$  for cleaning. Based on known test samples and the reproducibility of the results, the relative uncertainty in the cosurfactant con-

centrations was determined to be within  $\pm 5\%$ .

Assuming spherical W/O droplets with an aqueous core radius  $R_c$ , the ratio of the total water–oil interfacial area  $A_s$  to the aqueous volume  $V_m$  of the microemulsion is given as

$$\frac{A_s}{V_m} = \frac{(m_s/M_s) \cdot N_A a}{V_m} = \frac{4\pi R_c^2}{4/3 \pi R_c^3} = \frac{3}{R_c}, \quad (9)$$

where  $m_s$  and  $M_s$  are the surfactant mass and molar mass, respectively,  $N_A$  is Avogadro's number, and  $a$  the interfacial area of the surfactant molecule. By rearranging Eq. (9), one obtains an expression for the overall particle radius  $R$ :

$$R = \frac{3M_s V_m}{m_s N_A a} + l, \quad (10)$$

where  $l$  is the surfactant hydrocarbon chain length. The effective length of a C–C bond is approximately 1.25 Å, and thus the total length of the hydrophobic part of a straight SDS molecule is  $l = 1.5$  nm.

The average molecular interfacial area generally depends on the nature and concentration of the cosurfactant. However, since the latter dependence is diminished by the presence of salt,<sup>10</sup> we assumed  $a$  to be constant for all the samples. The interfacial molecular area was determined in a separate static and dynamic light scattering analysis on a series of diluted samples of one of the actual microemulsions (B8), prepared using the Shulman/Graciaa dilution procedure.<sup>11</sup> The numerical value was found to be  $a = 69 \pm 2 \text{ Å}^2$ , which is consistent with experimental values given in Ref. 10 for SDS micelles as a function of the concentration of present butanol, although slightly larger than that obtained by Cazabat and Langevin<sup>8</sup> who found  $a = 50 \text{ Å}^2$ .

In homodyne DLS the recorded quantity is the scattered intensity correlation function  $g^{(2)}(q, t)$ , related to  $g^{(1)}(q, t)$  through the Siegert relation<sup>7</sup>:

$$g^{(2)}(q, t) = 1 + b |g^{(1)}(q, t)|^2, \quad (11)$$

where the constant  $b$  is independent of time, but depends on the spatial and temporal coherence of the scattered light at the detector and thus on the correlation sample time.

In order to properly resolve the different time scales which appeared in the correlation data for some of the samples, the correlator was subdivided into eight separate sub-correlators, each scanning different time scales. In this so-called parallel mode, the complete correlation function of each sample may be covered in one run. Since the value of the experimentally determined coefficient  $b$  of Eq. (11) depends on sample time, and thus will be different for each subcorrelator, the stitching together of the subcorrelation functions is not trivial. In the Appendix we show that under certain con-

ditions, however, it may be easily accomplished. The validity of this procedure was further checked by examining the curve fitting residuals. The fittings were done using an iterative least square method.

#### IV. RESULTS AND DISCUSSION

Relevant microemulsion data for the samples used (labeled B0–B11) are given in Table I. We note that both droplet size and volume fraction increases with decreasing cosurfactant concentration. The scattered intensity autocorrelation functions of the three most dilute samples (B8, B9, B10) were found to be single exponential and proportional to  $q^2$ . Hence, this was interpreted to be due to translational diffusion of W/O droplets, and the effective diffusion coefficients  $D^{\text{eff}}$  were obtained by the use of Eq. (7). The droplet size polydispersities of these three samples were found to be very small, with typical values for  $\Gamma / \langle D^{\text{eff}} q^2 \rangle^{1/2}$  in the range 0.2–0.3, being close to the minimum degree of polydispersity detectable in DLS measurements.<sup>12</sup>

In the remaining microemulsions (B1–B7) however, components with much ( $\sim 10$  times) faster decays were observed in addition to the one expected from translational diffusion alone. For these samples a double, or even a triple exponential function had to be used to satisfactorily fit the data. As a typical example, we have in Fig. 1 shown three fits to the correlation data of sample B5 at  $\theta = 120^\circ$  using

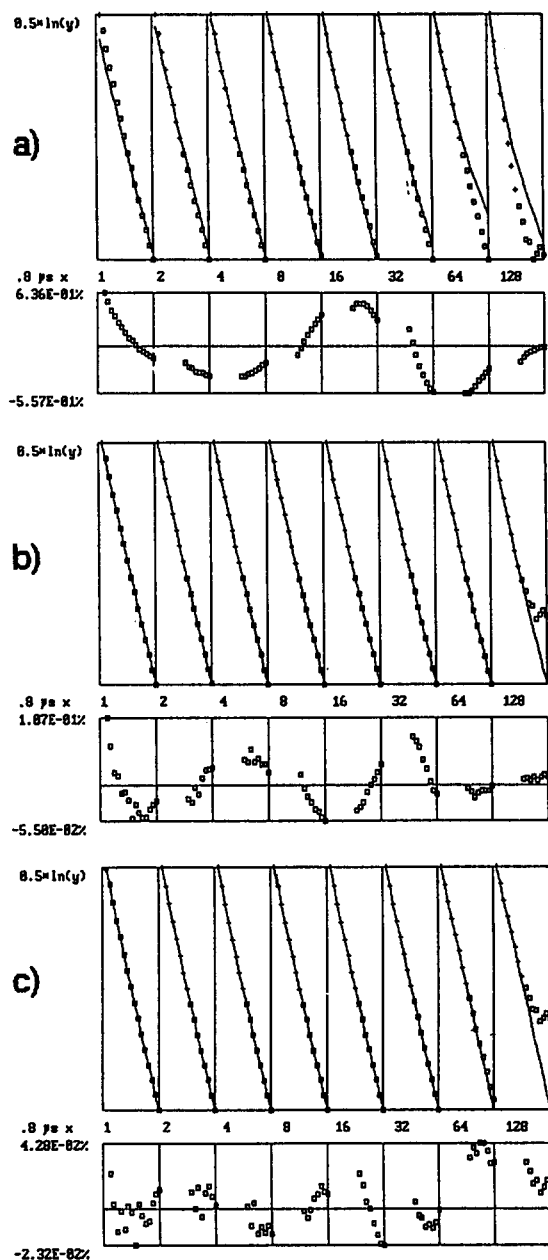
- A polydispersity broadened single exponential decay [Eq. (A5) with  $n = 1$ ]
- a polydispersity broadened double exponential decay [Eq. (A5) with  $n = 2$ ]
- a pure triple exponential decay [Eq. (A5) with  $n = 3$ ,  $\sigma = 0$ ].

As may be seen from the residuals [Fig. 1(c)], the data did not allow for any “polydispersial” triple exponential decay fit. We note that (c) is a better fit than (b), and hence in general we used the triple modal correlation function to fit the data. For each sample, the relative value of the amplitude ( $A_1$ ) of the slowest decay mode was found to contribute at least 70% to the total signal. The decay constant ( $\Gamma_1$ ) of this mode was found to be approximately proportional to  $q^2$ , and, as will be discussed beneath, was interpreted to be due to translational (effective) diffusion of the microemulsion droplets according to the relation  $D^{\text{eff}} = \Gamma_1 / q^2$ .

The amplitude ( $A_3$ ) of the fastest decay ( $\Gamma_3$ ) mode of the fitting was found to contribute at most 2% to the total signal. Since these components were expected also to contain contributions from photomultiplier afterpulsing, they were not further analyzed.

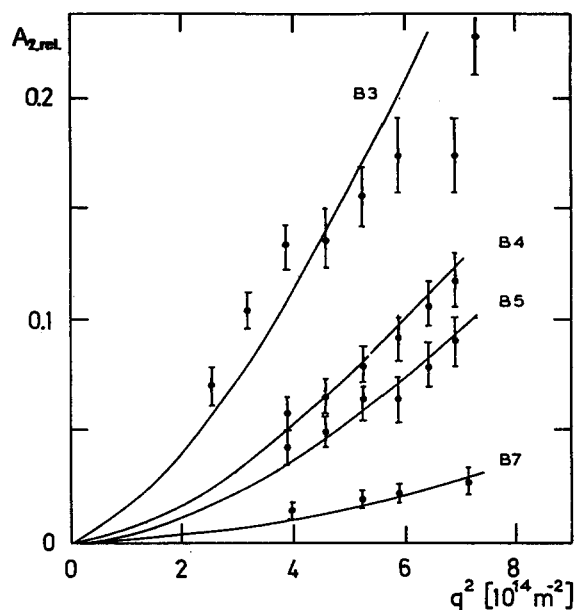
TABLE I. Basic sample data: Total cosurfactant concentration  $C_c$  (mass %) microemulsion droplet volume fraction  $\phi$  and geometrically obtained overall droplet radius  $R$ . The samples B0 and B1 are in the Winsor III (three phase) regime, while samples B2–B10 are Winsor II (microemulsion + excess brine).

Sample:	B0	B1	B2	B3	B4	B5	B6	B7	B8	B9	B10
$C_c$ (%):	2.34	2.46	2.50	2.60	2.80	2.90	3.10	3.24	3.40	4.00	5.00
$\phi$ :	0.500	0.410	0.375	0.335	0.270	0.250	0.235	0.210	0.200	0.180	0.150
$R$ (nm):	...	37.6	33.2	28.1	20.5	18.5	16.8	14.7	13.4	11.7	9.2



The relative amplitude ( $A_2$ ) of the intermediate mode was found to contribute 4%–25% to the total signal, and was generally observed to decrease with decreasing scattering angles. The decay constant ( $\Gamma_2$ ) of this mode was found to be almost  $q$  independent for the samples B7, B6, B5 and B4, and then increasingly  $q$  dependent for the samples B3, B2 and B1. This component of the correlation function shall be analyzed in the following section.

In Fig. 2 we have plotted the relative amplitude  $A_{2,rel} = A_2/(A_1 + A_2 + A_3)$  as a function of  $q^2$  for the sam-



ples B3, B4, B5 and B7. We notice that  $A_{2,\text{rel}}$  disappear in the  $q \rightarrow 0$  limit. This rules out the possibility that this mode is due to polydispersity fluctuations.<sup>12</sup> This fact, combined with the nearly  $q$  independence of  $\Gamma_2$  suggests that this mode instead is due to scatterers exhibiting rotations and/or flexing motions. Furthermore, these scatterers must be droplet *aggregates*, since individual microemulsion droplets are too small (as seen from Table I) to account for the relatively large  $A_{2,\text{rel}}$  values.

$$F_{\zeta}(q,t) = S_1(qL)e^{-D_0q^2t} + S_2(qL)e^{-(D_0q^2 + 6\theta_0)t}, \quad (12)$$

A second, independent value for the aggregate size may be obtained from the rotational diffusion coefficient  $\theta_0$  itself. Again assuming rod shaped aggregates we used Perrin's formula relating  $\theta_0$  to the radius  $R_{\text{aggr}}$  of the rod's major semiaxis<sup>7</sup>:

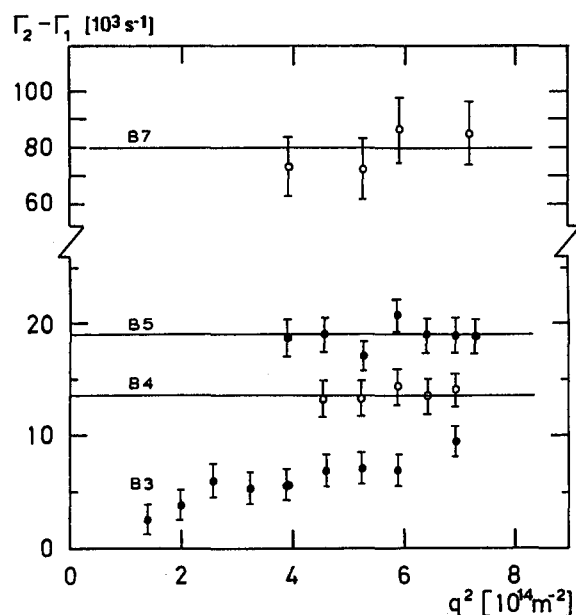


FIG. 3. The rotation/internal motion decay constant ( $\Gamma_2 - \Gamma_1$ ) vs  $q^2$  for the samples B3, B4, B5 and B7.

$$\theta_0 = \frac{3kT}{16\pi\eta R_{\text{aggr}}^3} \left\{ \frac{(2-\rho)G(\rho) - 1}{(1-\rho^2)} \right\}, \quad (13)$$

where  $\rho$  is the axial ratio (diameter/length) of the rod and

$$G(\rho) = \frac{1}{(1-\rho^2)^{1/2}} \ln \left\{ \frac{1 + (1-\rho^2)^{1/2}}{\rho} \right\}. \quad (14)$$

According to Eq. (12), the experimental value for  $\theta_0$  is obtained from the data by forming the expression  $(\Gamma_2 - \Gamma_1)/6$ . In Fig. 3 we have plotted  $(\Gamma_2 - \Gamma_1)$  vs  $q^2$  for the samples B3, B4, B5 and B7. Except for B3 ( $\varphi = 0.34$ ),  $(\Gamma_2 - \Gamma_1)$  is seen to be  $q$  independent, which indeed is what one expects for rotational modes [as seen from Eq. (13)], and as it turns

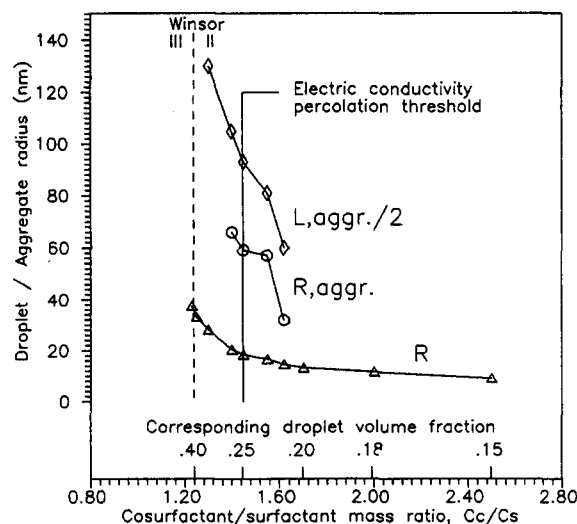


FIG. 4. Radii of microemulsion droplets and droplet aggregates versus the total cosurfactant concentration/corresponding droplet volume fraction. Also shown are the Winsor II  $\rightarrow$  III phase transition and the electrical conductivity percolation threshold.

out, for internal modes as well. Using  $\rho = R/R_{\text{aggr}}$ , we obtained  $R_{\text{aggr}}$  from Eq. (13) by iteration.

In Fig. 4 we have plotted the aggregate radii  $R_{\text{aggr}}$  and  $L_{\text{aggr}}/2$  as a function of the cosurfactant concentration ( $C_c/C_s$ ) and the corresponding droplet volume fraction  $\varphi$ .

We note that although the radii of the droplets themselves increase as the system moves from the far Winsor II towards the Winsor III region of the phase diagram, the aggregate radii increases even more rapidly, as one indeed should expect. In his analysis, Pecora<sup>7</sup> showed that rotational modes are detectable in DLS only for scatterers which satisfies the condition  $qL > 3$ . Thus, this is probably the reason why we do not observe any extra decays in the samples B8–B10.

Figure 4 further shows that the values for the size of the aggregates as estimated from the relative scattering amplitudes ( $L_{\text{aggr}}/2$ ) are larger (almost twice) than those obtained from the time decay constants ( $R_{\text{aggr}}$ ). This discrepancy may qualitatively be explained as follows: As a first approximation one may assume that droplet interactions correlate the relative *positions* of the aggregates, but not their *orientations*, i.e., that the scattering from the translational modes is partly coherent while that from the rotational modes is not. Indeed, static light scattering analysis showed the static structure factor  $S(q=0)$  to be less than unity for all the samples studied. This is also what one would expect in attractive/aggregating systems. Hence, the dynamic structure factor of the rotational mode, and thus the value of  $L_{\text{aggr}}$ , may be too large. Further, excluded volume effects will cause restricted rotation of the aggregates, thereby increasing the temporal decay of these modes,<sup>13</sup> and thus underestimate the value of  $R_{\text{aggr}}$ .

One may question the validity of using stiff rods as a model for the microemulsion aggregates. However, the two leading terms in the harmonic mode expansion of the scattering [Eq. (5)] are rather independent of the actual type of the internal aggregate dynamics. Indeed, interpreting the  $A_2$  amplitudes in terms of flexing Gaussian coils, and using the theory of Pecora,<sup>8</sup> gave values for the aggregate sizes quite similar to  $L_{\text{aggr}}$ . As for  $R_{\text{aggr}}$  a more realistic model would probably be to describe the aggregates in terms of worm-like,<sup>14</sup> perhaps even fractal structures. Since such descriptions introduce additional parameters (persistence lengths, fractal dimensions, etc.) the accuracy of our data did not allow for any numerical analyses of such models.

## B. Translational diffusion coefficients analysis

As discussed above, the dominating mode in the correlation function was interpreted to be due to translational motion of the scatterers, according to the relation  $D^{\text{eff}}(0) = \Gamma_1/q^2$ . The remaining  $q$  dependence of  $D^{\text{eff}}(q)$  was satisfactorily fitted by the following expression containing the lowest order  $q$ -dependent term:

$$D^{\text{eff}}(q) = D^{\text{eff}}(0)(1 + gq^2), \quad (15)$$

where the parameter  $g$  generally depends on sizes, interactions and polydispersity of the scatterers. Let us first however, consider the effective collective diffusion coefficient  $D^{\text{eff}}(0)$  in some detail.

In a dilute dispersion of interacting droplets,  $D^{\text{eff}}(0)$  may be expanded in terms of the droplet volume fraction about the free particle diffusion coefficient  $D_0$ <sup>15</sup>:

$$D^{\text{eff}}(0) = D_0[1 + \alpha\varphi + O(\varphi^2)], \quad (16)$$

where the diffusion virial coefficient  $\alpha$  is a function of the droplet interaction potential.

For a genuine hard-sphere system Felderhof<sup>20</sup> obtained the value  $\alpha = 1.56$ , whereas one for additional interactions, repulsive or attractive, expects larger or smaller (possibly negative) values, respectively. Both the size of the droplets (and thus  $D_0$ ), and the interaction between them (and thus  $\alpha$ ) however, vary as one moves from the Winsor II to the Winsor III regime. In order to extract the effect of the interactions alone, we computed for each sample the ratio  $D^{\text{eff}}(0)/D_0$ , which according to Eq. (16) is a measure of the deviation from free diffusion. Values for the free diffusion coefficients  $D_0$  were obtained using Eq. (4) by assuming the solvent viscosity to be that of pure cyclohexane, and the hydrodynamic radius  $R_H$  to be equal to the overall droplet radius  $R$  (Table I). In Fig. 5 the resulting  $D^{\text{eff}}(0)/D_0$  is plotted as a function of  $\varphi$ . As Fig. 5 indicates, there are only minor changes in the droplet interactions as one moves from the Winsor II into the Winsor III regime. This situation is quite different from that expected for a critical transition where the apparent droplet diffusion freezes, i.e., the ratio  $D^{\text{eff}}(0)/D_0$  approaches zero at the transition point.<sup>16</sup> Hence, for our particular microemulsion series the phase separation is definitely not critical.

This conclusion is further substantiated by the fact that  $D^{\text{eff}}(q)$  decreases with increasing  $q$  vector (see Fig. 6). This is in contrast to critical microemulsions (for example those containing pure butanol as cosurfactant<sup>16</sup>), where one expects,<sup>17</sup> and also observes<sup>16</sup>  $D^{\text{eff}}(q)$  to increase with increasing  $q$  vector.

The observed  $q$  dependence of  $D^{\text{eff}}$  also rules out inter-

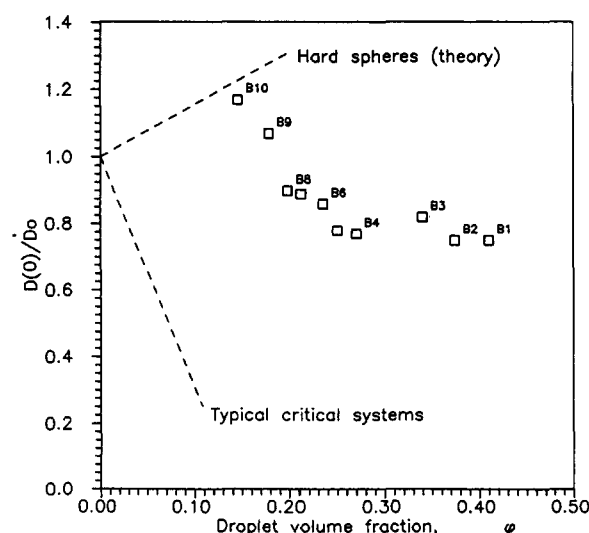


FIG. 5. Ratio of effective to free translational diffusion coefficient as a function of droplet volume fraction. The dashed curves corresponds to theoretical values for solutions of hard spheres (Ref. 15) and to experimental values for close-to-critical solutions (Ref. 16), respectively.

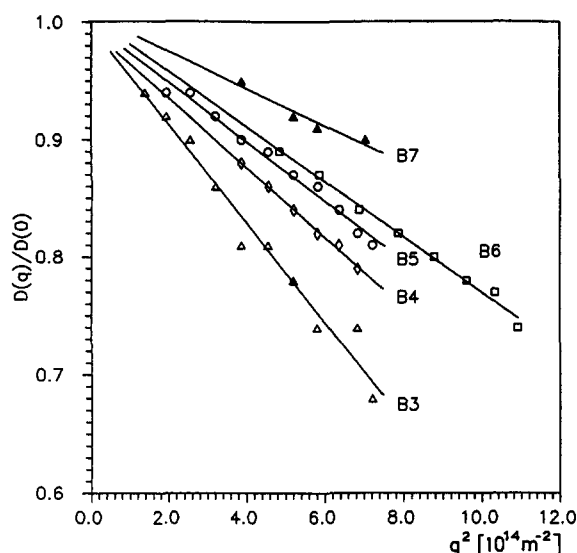


FIG. 6. Angular variation of the effective translational diffusion coefficient  $D^{\text{eff}}(q)$  for the samples B3–B7. The curves are least mean square fits to Eq. (15).

pretations in terms of droplet size polydispersity and eventual presence of dust in the samples, since these effects as well should cause  $D^{\text{eff}}$  to increase with increasing  $q$ .<sup>9</sup> We believe that the observed  $q$  dependence of  $D^{\text{eff}}$  is due to droplet interactions, which formally may be taken into account by writing<sup>18</sup>:

$$D^{\text{eff}}(q) = D_0 H(q)/S(q). \quad (17)$$

Here, the factor  $H(q)$  and the static structure factor  $S(q)$  describes hydrodynamic and direct droplet interactions, respectively, and hence the actual sign of the  $q$  dependence is determined by the interplay of these two factors. We note that detailed theoretical<sup>19,20</sup> and experimental<sup>21</sup> studies have shown that for hard sphere systems at moderate volume fractions one should indeed expect a negative  $q$  dependence. The reason why one in general does not observe such a behavior in microemulsions is that the sizes of the droplets are usually too small. This has also been noted by Guest and Langevin,<sup>22</sup> who recently observed a similar angular dependence of the translational diffusion coefficient in a microemulsion with microstructure sizes in the same range as ours. They did not, however, report any observations of multiexponential correlation functions.

### C. Multiple scattering

Some of the samples were observed to be quite strong scatterers. The transmission coefficient of the samples were found to be approximately 0.85 (B1), 0.90 (B2 and B3) and  $> 0.95$  for the others. Except perhaps for samples B1–B3 we believe that multiple scattering is not responsible for any of the observed effects for the following reasons:

- we know of no mechanism in which multiple scattering introduces a splitting of the correlation function into different decay modes
- the amplitudes  $A_2$  of the decay modes were found to be



orders of magnitude larger than those expected from double scattering, which should be the main contribution to multiple scattering

—a distinct feature of multiple scattering in DLS was missing in our measurements, at least for the samples B4–B10, namely the *apparent* divergence of  $D^{\text{eff}}$  in the forward ( $q = 0$ ) scattering direction. However, the observed nonvanishing value of  $A_2$  as  $q \rightarrow 0$  for sample B3 (see Fig. 2), and particularly for B1 and B2 (not shown in the figure) for which  $A_{2,\text{rel}}$  definitely did not disappear in the forward scattering direction, may just be due to this multiple scattering forward scattering divergence.

## V. CONCLUSIONS

We have performed dynamic light scattering analysis of a Winsor type microemulsion system, containing a mixture of 1-butanol and 1-pentanol as cosurfactant. By decreasing the total cosurfactant concentration this system was transformed from a microemulsion of separated water-in-oil droplets in coexistence with an excess water phase (Winsor II), into a microemulsion in coexistence with both an aqueous and a hydrocarbon excess phase (Winsor III). This transition seems to start out as an aggregation of the microemulsion droplets, and takes place far from any critical points. The latter is in contrast to systems containing pure butanol as the cosurfactant.

The presence of aggregation was primarily inferred from the observation of additional decay modes in the scattered intensity autocorrelation data. Values for the aggregate sizes were obtained in two ways: one,  $R_{\text{aggr}}$  from the decay time  $\Gamma_2$ , and another  $L_{\text{aggr}}$  from the relative amplitude  $A_{2,\text{rel}}$  of the additional mode. These values were shown to be mutually consistent, and further also consistent with the translational diffusion coefficient of the scatterers. Although aggregation of microemulsion droplets has earlier been observed using neutron scattering,<sup>23</sup> fringe pattern photobleaching recovery<sup>24</sup> and electric birefringence<sup>25</sup> methods, the present work is to our knowledge the first such observation by dynamic light scattering.

Finally, we would like to mention that the aggregation hypothesis also appears to be consistent with the electric conductivity percolation transition observed for this microemulsion system. In another set of experiments we found the percolation threshold to be  $\varphi_T = 0.25$ , and thus far from the phase separation itself which occurs at  $\varphi = 0.40$  (see also Fig. 4). In contrast, in close-to-critical microemulsion systems such as those reported by Cazabat *et al.*<sup>16</sup> these transitions seem to occur on top of each other, and moreover, at significantly lower volume fractions ( $\varphi < 0.15$ ). We intend to report on these experiments in a future paper.

## ACKNOWLEDGMENT

This work was partly supported by STATOIL.

## APPENDIX: PARALLEL CORRELATION FUNCTIONS ANALYSIS

To properly cover the different time scales contained in a multiexponential correlation function, one may operate

the correlator in so-called parallel mode. The correlator is then divided into eight separate subcorrelators, each containing 16 channels. The sample time of subcorrelator  $i + 1$  is set equal to  $m$  times that of subcorrelator  $i$  ( $m = 2, 3, \dots, 8$ ). In this way each subcorrelator scans different time scales, and the subcorrelation functions taken together may then cover the total time span of interest. Thus, by properly choosing the *fundamental* sample time  $T_s$  (sample time of subcorrelator no. 1) the total correlation function of a sample can be recorded in a single run.

In the present work the total correlation function was constructed by stitching together the content of the subcorrelators, incorporating from subcorrelator  $i + 1$  only those channels not overlapping any channels of subcorrelator  $i$ . However, the constant factor  $b$  of Eq. (8) will in general depend on sample time, i.e., differ from one subcorrelator to the next. We have analyzed the situation by assuming a Lorentzian spectrum of the scattered light when, according to Jakeman,<sup>22</sup> the factor  $b_i$  of subcorrelator  $i$  may be expressed as

$$b_i = b_0 \left[ \frac{\sinh(\Gamma m^{i-1} T_s)}{\Gamma m^{i-1} T_s} \right]^2, \quad (\text{A1})$$

where the constant  $b_0$  is independent of both sample time ( $m^{i-1} T_s$ ) and the decay constant. Taking the ratio of the  $b$ 's for two neighboring subcorrelators, and expanding to lowest order one gets

$$\frac{b_{i+1}}{b_i} = 1 - \frac{1}{3} \left( 1 - \frac{1}{m^2} \right) (\Gamma m^i T_s)^2 + \dots \quad (\text{A2})$$

Hence, significant overlapping misfits in the junction between the subcorrelators  $i$  and  $i + 1$  are not expected if  $\Gamma m^i T_s \ll 1$ .

The *exponential* part of Eq. (8) for subcorrelator  $i$  takes the form

$$|g^{(1)}(q, n_i m^{i-1} T_s)|^2 \approx \exp(-2\Gamma n_i m^{i-1} T_s), \quad (\text{A3})$$

where  $n_i$  is the channel number of subcorrelator  $i$ ;  $n_i = (1, 2, 3, \dots, 16)$ . At the junction between subcorrelator  $i$  and  $i + 1$  one has  $n_i = 16$ .

By allowing  $b_{i+1}/b_i$  to deviate maximum 2% from unity, and inserting the corresponding value for  $\Gamma m^i T_s$  into Eq. (A3), one obtains  $(g^{(1)}(q, t))^2 = 0.011$  and 0.06 for  $m = 2$  and 3, respectively. Thus, by the time  $b_{i+1}$  starts to deviate appreciably from  $b_i$ , the correlation function is almost decayed out. This was also confirmed in the curve fittings. Moreover, by optionally correcting the content of each subcorrelator using Eq. (A1) (with an averaged  $\Gamma$ ), the results were not significantly altered.

The long time scales involved in the parallel mode operation of the correlator makes the cumulant expansion treatment of particle size polydispersity [Eq. (9)] no longer valid. One may then instead consider each decay constant to be broadened with a square distribution with half width  $\Delta\Gamma_i = \sigma\Gamma_i$ . In order to keep the number of fitting parameters low we used a common value of  $\sigma$  to describe all the decay modes:



$$g^{(1)}(q,t) = \frac{\int_{\Gamma-\Delta\Gamma}^{\Gamma+\Delta\Gamma} e^{-\Gamma t} d\Gamma}{\int_{\Gamma-\Delta\Gamma}^{\Gamma+\Delta\Gamma} d\Gamma} = e^{\Gamma t} \frac{\sinh(\Delta\Gamma t)}{\Delta\Gamma t}. \quad (\text{A4})$$

Decay broadening may then optionally be taken into account in the analysis by fitting to the data a polydisperse version of Eq. (6):

$$g^{(1)}(q,t) = \sum_{i=1}^n A_i e^{-\Gamma_i t} \frac{\sinh(\sigma\Gamma_i t)}{\sigma\Gamma_i t}, \quad (\text{A5})$$

where  $A_i$  is the amplitude of the  $i$ th mode.

<sup>1</sup>Microemulsions, *Theory and Practice*, edited by L. M. Prince (Academic, New York, 1977).

<sup>2</sup>P. A. Winsor, *Trans. Faraday Soc.* **44**, 376 (1948).

<sup>3</sup>L. E. Scriven, *Nature* **263**, 2984 (1976).

<sup>4</sup>D. Langevin, *Phys. Scr.* **13**, 252 (1986).

<sup>5</sup>*Surface Phenomena in Enhanced Oil Recovery*, edited by D. O. Shah (Plenum, New York, 1981).

<sup>6</sup>A small collection of proceedings containing light scattering studies of microemulsions: *Micellization, Solubilization and Microemulsions*, edited by K. L. Mittal (Plenum, New York, 1977); *Microemulsions*, edited by I. D. Robb (Plenum, New York, 1982); *Surfactants in Solutions*, edited by K. L. Mittal and B. Lindman (Plenum, New York, 1984). *Microemulsion Systems*, edited by H. L. Rosano and M. Clause (Dekker, New York,

1986); *Surfactants in Solution*, edited by P. Bothorel and K. L. Mittal (Plenum, New York, 1986).

<sup>7</sup>B. J. Berne and R. Pecora, *Dynamic Light Scattering* (Wiley, New York, 1976).

<sup>8</sup>A. M. Cazabat and D. Langevin, *J. Chem. Phys.* **74**, 3178 (1981).

<sup>9</sup>P. N. Pusey and R. J. A. Tough, in *Dynamic Light Scattering—Applications of Photon Correlation Spectroscopy* (Plenum, New York, 1985).

<sup>10</sup>M. Almgren and S. Swarup, *J. Phys. Chem.* **86**, 4212 (1982).

<sup>11</sup>A. Graciaa, J. Lachaise, M. Martinez, M. Bourrel, and C. Chambu, *C. R. Acad. Sci. Paris Ser. B* **282**, 547 (1976).

<sup>12</sup>P. N. Pusey and W. van Megen, *J. Chem. Phys.* **80**, 3513 (1984).

<sup>13</sup>C. C. Wang and R. Pecora, *J. Chem. Phys.* **72**, 5333 (1980).

<sup>14</sup>S. R. Aragón S and R. Pecora, *Macromolecules* **18**, 1868 (1985).

<sup>15</sup>B. U. Felderhof, *Physica* **89A**, 373 (1977).

<sup>16</sup>A. M. Cazabat, D. Langevin, J. Meunier, and A. Pouchelon, *J. Phys. Lett.* **43**, L-89 (1982); A. M. Cazabat, D. Chatenay, D. Langevin, and J. Meunier, *Faraday Discuss. Chem. Soc.* **76**, 291 (1983).

<sup>17</sup>K. Kawasaki, *Phys. Lett.* **30 A**, 325 (1969); *Ann. Phys. N.Y.* **61**, 1 (1970); *Phys. Rev. A* **1**, 1750 (1970).

<sup>18</sup>H. M. Fijnaut, C. Pathmananoharen, E. A. Nieuwenhuis, and A. Vrij, *Chem. Phys. Lett.* **59**, 351 (1978).

<sup>19</sup>I. Snook, W. van Megen, and R. J. A. Tough, *J. Chem. Phys.* **78**, 5825 (1983).

<sup>20</sup>C. W. J. Beenakker and P. Mazur, *Phys. Lett. A* **98**, 22 (1983).

<sup>21</sup>W. van Megen, R. H. Ottewill, S. M. Owens, and P. N. Pusey, *J. Chem. Phys.* **82**, 508 (1985).

<sup>22</sup>D. Guest and D. Langevin, *J. Coll. Int. Sci.* **112**, 208 (1986).

<sup>23</sup>R. Ober and C. Taupin, *J. Phys. Chem.* **84**, 2418 (1980).

<sup>24</sup>D. Chatenay, W. Urbach, A. M. Cazabat, and D. Langevin, *Phys. Rev. Lett.* **54**, 2253 (1985).

<sup>25</sup>P. Guèring, A. M. Cazabat, and M. Paultette, *Europhys. Lett.* **2**, 953 (1986).